Direct electrosynthesis of poly-o-phenylenediamine bulk materials for supercapacitor application

Meirong Wang [a], Huaihao Zhang [a], Chengyin Wang [a,*], Xiaoya Hu [a], Guoxiu Wang [b,**]

[a] College of Chemistry and Chemical Engineering, Jiangsu Key Laboratory of Environmental Engineering and Monitoring, Yangzhou University, 180 Si-Wang-Ting Road, Yangzhou 225002, China
[b] Department of Chemistry and Forensic Science, University of Technology, Sydney, City Campus, Broadway, Sydney, NSW 2007, Australia

ARTICLE INFO

ABSTRACT

For the first time, poly-o-phenylenediamine (PoPD) bulk material was electrochemically synthesized using an electrochemical method. Sodium dodecyl sulfate (SDS) was added to o-phenylenediamine (oPD) solution and PoPD with different morphologies were obtained. The as-prepared materials were applied as the electrode materials in supercapacitors. The specific capacitance (SC) of the resultant PoPD was determined to be $106.4 \, F \, g^{-1}$ in $1 \, mol \, L^{-1}$ KNO_3 electrolyte from CV test. The electrochemical stability of PoPD electrode was investigated by charging and discharging the electrode for 1000 times in the potential range of -0.2 to $0.6 \, V$ versus SCE at the current density of $500 \, mA \, g^{-1}$. The electrode exhibits a good cycling stability, retaining up to 82% of its initial specific capacitance at 1000th cycle. This novel technique enables PoPD non-film material for supercapacitor application.

1. Introduction

Conductive oligomers and polymers have been the subject of considerable attention in past decades due to their electrical, optical and electrofluorescence attributes [1], and their potential applications in electrode material, microelectronics technology and corrosion inhibitors [2–4]. Polyaniline (PANI) is one of the most researched conducting polymers [5,6] because of its facile synthesis and environmental stability in the doped form. Polyaniline also has wide-ranging electrochemical properties which can be controlled by changing its oxidant and protonation states [7]. So far, micelle, surfactant, liquid crystal and mercapto-cyclodextrin have been employed in the synthesis of conducting polymers [8,9]. Interfacial synthesis and dilute polymerization have been also used in the preparation of polyaniline nanomaterials [10,11]. However, PANI is insoluble in common organic solvents due to the rigidity of aniline skeleton and hydrogen bonds of the adjacent amino groups [12,13]. In order to overcome the shortcomings of polyaniline in the plasticity, the polymers of aniline derivatives have also been extensively studied for their potential application as the substitute for polyaniline [14]. In recent years, aromatic diamine polymers have emerged as an alternative for conducting polymers with more active free

amino and imino groups which can be re-modified. The application of poly(p-phenylenediamine) and poly(m-phenylenediamine) in supercapacitor have been reported. Jaidev et al. employed p-phenylenediamine to form nanocomposite with grapheme sheets in acidic medium, and the resultant product was applied as electrode material for supercapacitor with the specific capacitance of $248 \, F \, g^{-1}$ [15]. Chen et al. adopted p-phenylenediamine to activate graphene which was meanwhile covered by p-phenylenediamine, and the product was applied in supercapacitor to yield the specific capacitance of $122 \, F \, g^{-1}$ [16]. PoPD is an aromatic polymer with 2,3-diaminophenazine or quinone ring structural units, showing high thermal stability [17]. oPD is one of the aniline derivatives and the preparation of PoPD can be achieved by the substitution of hydrogen with amino group, resulting in different molecular structure and characteristics from PANI [18]. Therefore, PoPD is a widely used material for electrode modification, electrocatalysis, sensors [19,20], corrosion inhibitor, and electrochromic-film technology [21,22]. An Au/poly(o-phenylenediamine) electrode has been selected by Martinusz et al. [23] and Ujvári et al. [24] as a model system for the studies of the low-frequency pseudocapacitance of conducting polymer electrodes. However, the capacitive behavior of PoPD has not been extensively studied.

There are two methods to synthesize PoPD: chemical method and electrochemical method. In the chemical method, PoPD is synthesized by reacting oPD monomer with an oxidant. Wang et al. prepared rose-like microstructure of $PoPD/Fe_2O_3$ composite by stirring $Fe_2(SO_4)_3$ and oPD vigorously at room temperature [25]. Large microfibrils were prepared by Sun et al. [26] on a large

* Corresponding author. Tel.: +86 514 87888454; fax: +86 514 87975244.
** Corresponding author. Tel.: +61 2 95141460; fax: +61 2 95141741.
E-mail addresses: wangcy@yzu.edu.cn, yzswcy@yzcn.net (C. Wang),
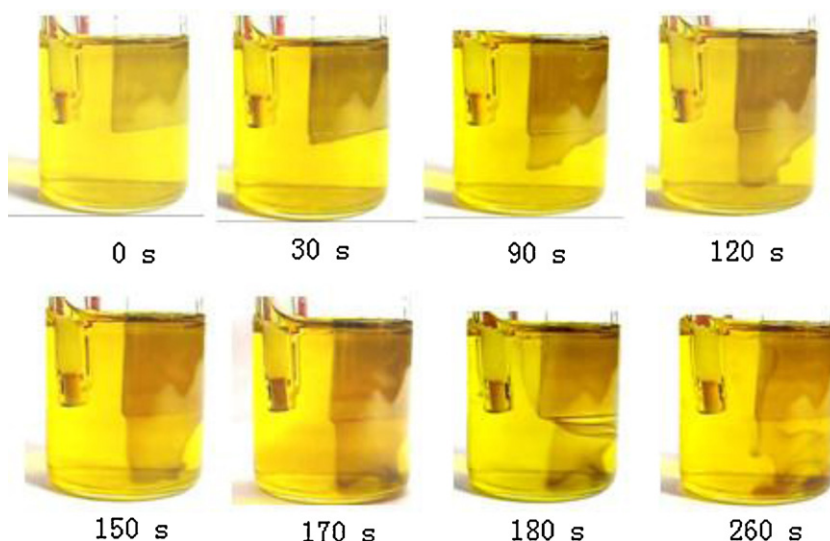Guoxiu.Wang@uts.edu.au (G. Wang).

Fig. 1. The process of electrochemical synthesis of PoPD without surfactant. The potential range is 0–1 V, and the scan rate is 50 mV s^{-1}.

scale with directly mixing aqueous ferric chloride and oPD solutions under ambient condition. The formation of such microfibrils is attributed to the self-assembly of the oPD dimers generated by the oxidation of oPD monomers by ferric chloride. Wang et al. [27] prepared PoPD using CuSO$_4$ as an oxidant at room temperature to react with oPD monomer. AgNO$_3$ was employed as the oxidant by Sun et al. [28] to react with oPD and PoPD microfibrils were yielded. This is a two-step process. Initially, oPD was oxidized by AgNO$_3$ to produce oligomers which then formed microfibril structure. Sun et al. [29] also prepared PoPD nanobelts by mixing HAuCl$_4$ and oPD at pH 7.5. Chemical synthesis is rapid and can produce large quantity materials. However, this method has several disadvantages, such as the high cost of gold and silver compound, the environmental pollution, and the tedious after-reaction process to remove the metal particles reduced in the reaction.

To date, PoPD prepared by electrochemical method is mainly film material deposited on the electrode surface. Wang et al. [30] obtained PoPD film on the electrode surface with cyclic voltammetry in the presence of Cu (II)–EDTA, and the Cu (II)–EDTA was then removed. The prepared electrode was successfully applied in the detection of Cu (II)–EDTA, and a higher sensitivity was yielded. Zane et al. [31] adopted an ionic liquid as the electrolyte, and electrochemical polymerization was carried out to yield PoPD film with good permeability and selectivity. The obtained electrode was used as the matrix to immobilize glucose oxidase and to prepare the biosensor which was of high sensitivity and excellent stability. Pisarevskaya et al. [32] used gold, platinum disc electrode, ITO conductive glass and SnO$_2$ electrode as the working electrode to synthesize soluble oligomer film and solid film of PoPD by cyclic voltammetry in 1 mol L^{-1} H$_2$SO$_4$ electrolyte in a three-electrode system. Chirizzi et al. [33] modified a glassy carbon electrode with PoPD film, and urease was immobilized subsequently on the film. The as-prepared electrode was applied in the detection of urea as a biosensor.

The product of electrochemical synthesis has so far been largely film materials. There are rare reports on the preparation of solid material in large quantity. Even for the electrodeposited film, its characterization requires scraping it off the electrode surface. The template-less electrochemical method for the direct preparation of non-film material has not been reported. In this work, cyclic voltammetry was employed for the direct synthesis of PoPD microbelt rather than films in the potential range of 0–1 V at the scan rate of 50 mV s^{-1}. The morphology of the resultant material could be regulated by the addition of surfactant. This method provides a new

technique for high-volume and continuous electrochemical synthesis of PoPD. Besides, there is no report about the application of chemically synthesized PoPD non-film materials. PoPD was applied as the electrode materials in electrochemical supercapacitor and promising results were obtained. The synthesis of PoPD non-film material with this method is facile, simple, and cost effective.

2. Experimental

2.1. Apparatuses and reagents

o-Phenylenediamine (CP), potassium nitrate (AR) and sodium dodecyl sulfate (AR) are purchased from Sinopharm Chemical Reagent Co., Ltd. The other reagents were of analytical grade. All reagents were used as received without further purification. The water used was purified through a Millipore system.

The synthesis and electrochemical tests were carried out on Modulab (Solartron Analytical). An indium tin oxide (ITO) glass slide purchased from Zhuhai Kaivo Electronic Components Co., Ltd. was employed as the working electrode for the polymerization. 85-1 magnetic stirrer was purchased from Nanjing Cole equipment Co., Ltd. SEM measurements were conducted on an S-4800II FESEM (Hitachi High-Technologies Corporation, Japan) at an accelerating voltage of 20 kV. UV–vis experiment was conducted on UV-visible (UV-Vis) spectrophotometer (Shimadzu, Japan) with the scanning wavelength ranging from 280 nm to 900 nm, and an EMLP microscope (Leica, Germany) was employed for the characterization. Gel permeation chromatography (GPC) instrument was used to investigate the molecular weight of the product with a Shimadzu GPC-802D gel column and a SPD-M10AVP detector, and the eluent of dimethylformamide at a flow rate of 1 mL min^{-1} was adopted.

2.2. Electrochemical synthesis of PoPD

Electrochemical polymerization was carried out on a three-electrode system using cyclic voltammetry in the presence and absence of the surfactant SDS. A video of the synthesis is presented in supplementary materials from which the preparation of PoPD can be observed. Fig. 1 shows the pictures of the synthesis process at different time. Initially, the solution was transparent; at 30 s precipitate appeared like cloud at the edge of the ITO glass slide; the black precipitate accumulated with the time and at 90 s it deposited on the bottom of the beaker.
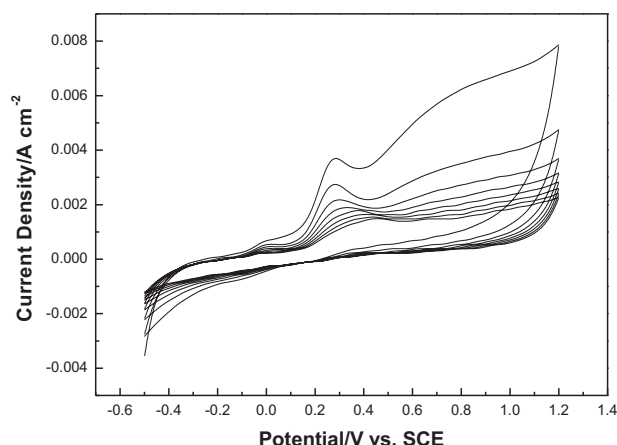
Fig. 2. Voltammogram obtained in $0.05\,mol\,L^{-1}$ oPD monomers containing $0.5\,mol\,L^{-1}$ KCl. The scan rate is $50\,mV\,s^{-1}$.

Supplementary data associated with this article can be found, in the online version, at http://dx.doi.org/10.1016/j.electacta.2012.12.087.

2.2.1. Synthesis of PoPD without surfactant

20 mL $0.05\,mol\,L^{-1}$ oPD solution containing $1.0\,mol\,L^{-1}$ KCl was placed in a beaker. ITO glass slide was ultrasonically cleaned with distilled water and ethanol, and then air-dried at room temperature. The ITO glass was used as the working electrode. The platinum foil electrode and saturated calomel electrode (SCE) were employed as counter electrode and reference electrode, respectively. The synthesis was conducted in the potential range of 0–1.0 V at a scan rate of $50\,mV\,s^{-1}$. A large quantity of precipitate was observed and the solution was removed by centrifugation. The precipitate was dried under the constant temperature of 60 °C for 5 h to yield red-brown solid for further characterization.

2.2.2. Synthesis of PoPD with the surfactant of SDS

30 mL of $0.05\,mol\,L^{-1}$ oPD containing $1.0\,mol\,L^{-1}$ KCl was added in five beakers. Then 0.06 g, 0.08 g, 0.1 g, 0.12 g, and 0.14 g SDS were added in above mentioned beakers, respectively. The polymerization and purification process were the same as the treatment of PoPD without SDS. The synthetic products were labeled as PoPD (a), PoPD (b), PoPD (c), PoPD (d) and PoPD (e).

2.3. Structural characterization of PoPD

FT-IR experiment was carried out on a BRUKER SENDOR 27 Infrared Spectrometer in the wave number range of $400–4000\,cm^{-1}$. UV-vis experiment was conducted on UV-visible (UV-Vis) spectrophotometer (Shimadzu, Japan) with the scanning wavelength ranging from 280 nm to 900 nm, and the samples were
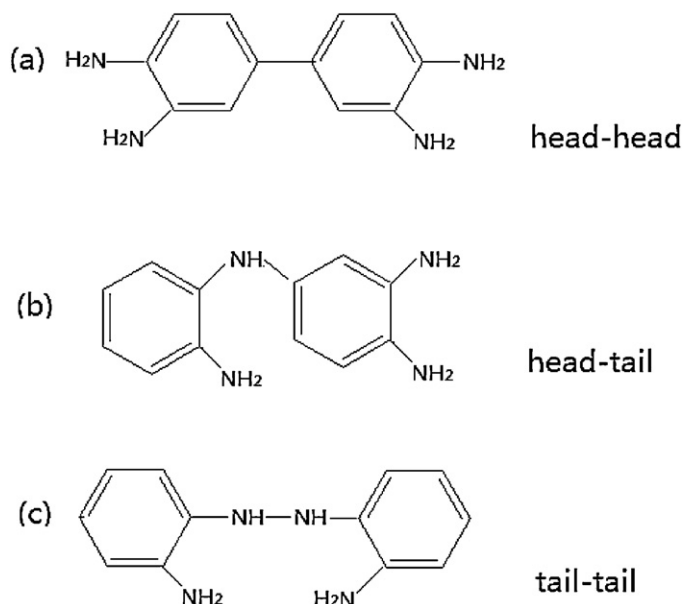
Scheme 1. Three structures of oPD dimmers.

dissolved in DMF to measure. SEM measurements were carried out on an S-4800II TESEM at an accelerating voltage of 20 kV.

2.4. Electrochemical test

2.4.1. Preparation of the supercapacitor

The three-electrode system was assembled with a working electrode, a counter electrode and a reference electrode. The mass ratio of active material, namely, PoPD, graphite and polytetrafluoroethylene (PTFE) was 7:2:1. They were mixed in the presence of ethanol to obtain the slurry which was then pasted on the surface of $1\,cm \times 1\,cm$ foamed nickel to form the working electrode. Activated carbon was employed to prepare the counter electrode according to above mentioned method. The obtained electrodes were heat treated at 80 °C overnight and pressed under the pressure of 10 MPa.

2.4.2. Supercapacitance measurement

The electrochemical properties were examined by the cyclic voltammetry (CV) and galvanostatic charge–discharge technique on an electrochemical workstation. CV measurement was performed over the potential range of −0.2 V to 0.6 V in $1\,mol\,L^{-1}$ KNO_3 at the scan rates of 5, 10, 30, 50 and $100\,mV\,s^{-1}$. The charge–discharge measurement was conducted in the potential range of −0.2 V to 0.6 V at the current density of 300, 500, 1000, 2000, and $5000\,mA\,g^{-1}$.
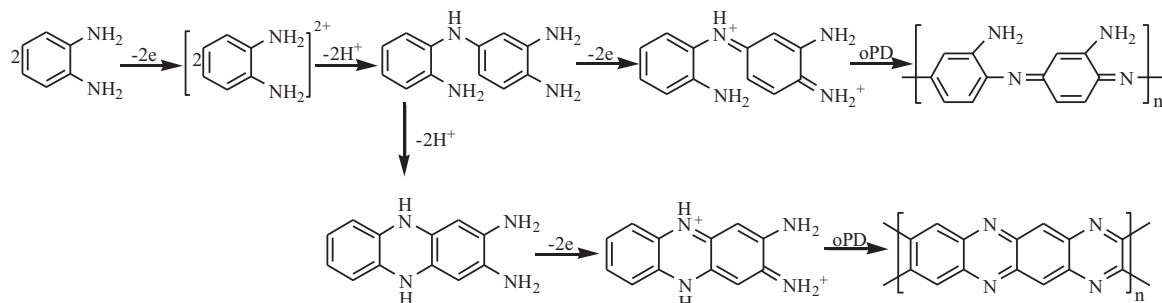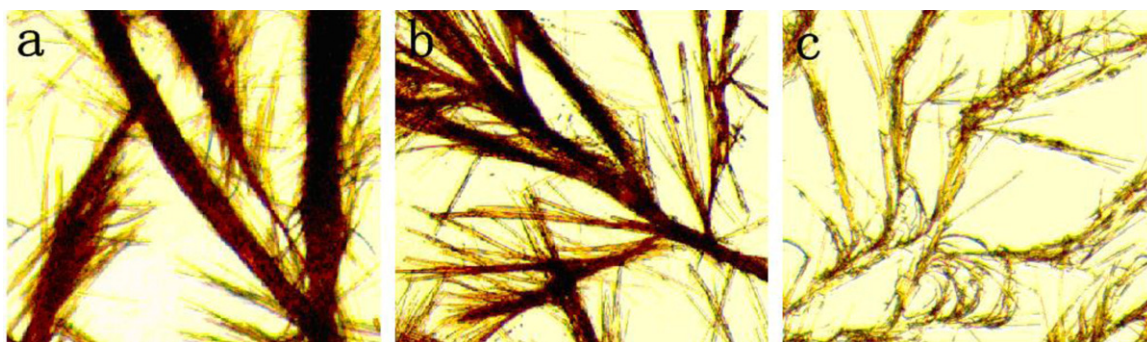

Scheme 2. Electropolymerization of oPD.

Fig. 3. Microscope image of the products synthesized at the scan rates of (a) 80 mV s^{-1}, (b) 50 mV s^{-1} and (c) 30 mV s^{-1} with 0.05 mol L^{-1} oPD containing 4 g L^{-1} SDS.

2.4.3. Cycle life test of the supercapacitors

The stability of the prepared capacitors can be examined by conducting repeated charge–discharge experiment. The capacitor was charged and discharged between −0.2 and 0.6 V in 1 mol L^{-1} KNO$_3$ solution over 1000 cycles to investigate the stability.

3. Results and discussion

3.1. Mechanism of electrochemical polymerization

Most literature concerned about the electrochemical polymerization of oPD in acidic conditions, while the electropolymerization under neutral conditions are rarely reported. In this experiment, the process of polymerization of PoPD was investigated in the potential range of 0–1.0 V. In order to conduct a more comprehensive study of the synthesis of PoPD, the potential range was extended to −0.5 to 1.2 V, and the cyclic voltammogram was shown in Fig. 2.

Obviously, there are two oxidative peaks. One is at the potential of 0.05 V which corresponds to the oxidation of oPD to form dimers. The dimer obtained by this process could have three possible structures [34], i.e. the head–head structure, head–tail structure and tail–tail structure, as shown in Scheme 1.

And head–tail structure is dominant among these structures [35]. The other oxidative peak appeared at 0.35 V is associated with the formation of long-chain PoPD by further oxidation of obtained head–tail dimers. Scheme 2 describes this process in which the PoPD formed could be linear structure and 1,4-substituted benzenoid–quinoid structure.

3.2. Effects of scan rates on electrochemical synthesis

In order to investigate the influence of scan rates on the morphology, different scan rates were applied in the electrochemical polymerization of 0.05 mol L^{-1} oPD containing 4 g L^{-1} SDS. The products were characterized to find the fact that the change of scan rates brought no significant influence on the overall morphology. Fig. 3 shows the microscope characterized image of PoPD synthesized in 80, 50 and 30 mV s^{-1} with 4 g L^{-1} SDS, which indicates that the "branches" of the tree-like product becomes finer with the decrease of scan rate. It could be explained by that at high scan rate, oPD radicals yielded from the oxidation of oPD were pushed to the anode with the flux of oPD molecules and were further oxidized to obtain cations. The amount of oPD radicals used to form dimers decreased drastically, leading to less polymerization reaction sites and thick "braches". This is consistent with the results reported in the literature [36].

3.3. FT-IR characterization

As is discussed, there are two structures of PoPD. FT-IR characterization was conducted to further confirm the structure of as-prepared PoPD. Fig. 4 shows the FT-IR spectrum of PoPD synthesized under different conditions.

Fig. 4a corresponds to the product synthesized without SDS. Two peaks at 3222 cm^{-1} and 3143 cm^{-1} are ascribed to the N—H stretching vibration. The peak at 3078 cm^{-1} is attributable to the C—H. Peaks at 771 cm^{-1} and 613 cm^{-1} can be assigned to the C—H out-of-plane bending vibration of benzene ring in phenazine units.
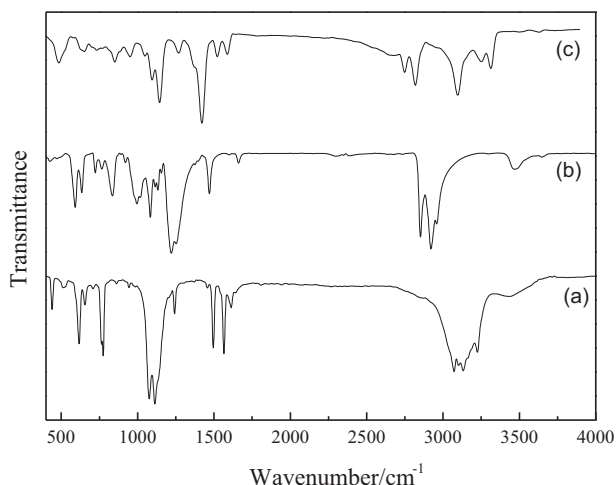

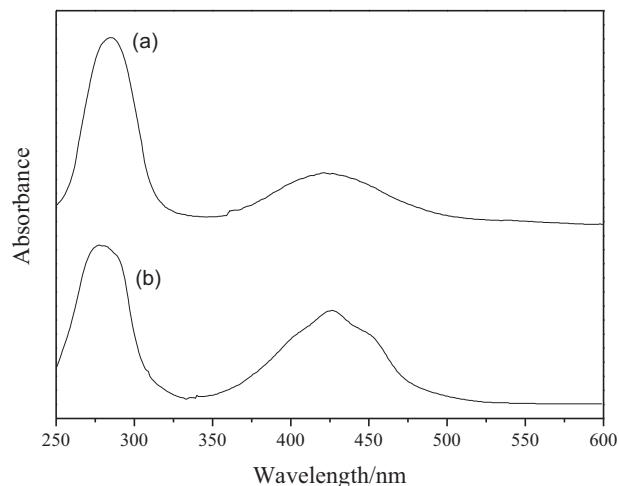**Fig. 4.** FT-IR spectra of surfactant-free (a) PoPD, (b) SDS and (c) PoPD (c).

Fig. 5. UV–vis image of the product; (a) and (b) correspond to surfactant-free PoPD and PoPD (c).
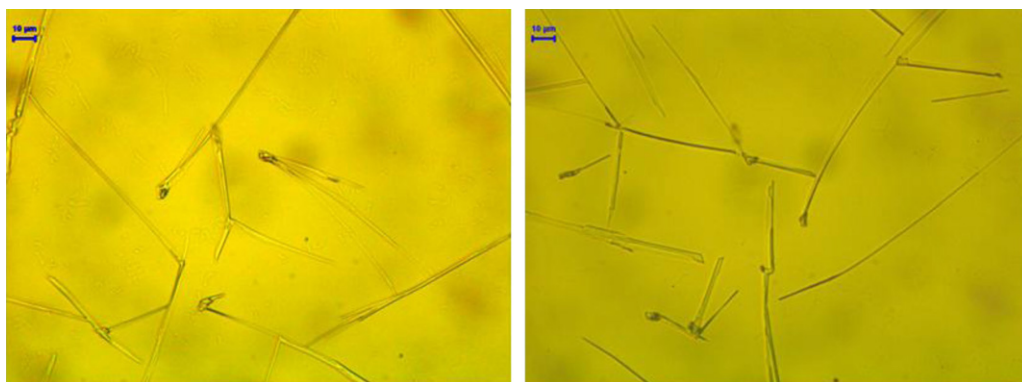
Fig. 6. Optical microscope images of PoPD prepared without SDS (dimensional scale 10 μm).

Two peaks at 1573 cm^{-1} and 1616 cm^{-1} suggest the C=C and C=N bending vibration, respectively, indicating the formation of PoPD. The peak at 1085 cm^{-1} is ascribed to the stretching vibration of C–N connected to benzene units. Fig. 4b is the FT-IR curve of SDS presented to compare with the curve of PoPD (c) which is shown

in Fig. 4c. The FT-IR results yielded from the products in the presence and absence of SDS were compared, and it could be observed from the curves that the presence of SDS during the electropolymerization process introduced the shift and decrease of original PoPD peaks and more peaks from SDS. It could be observed that
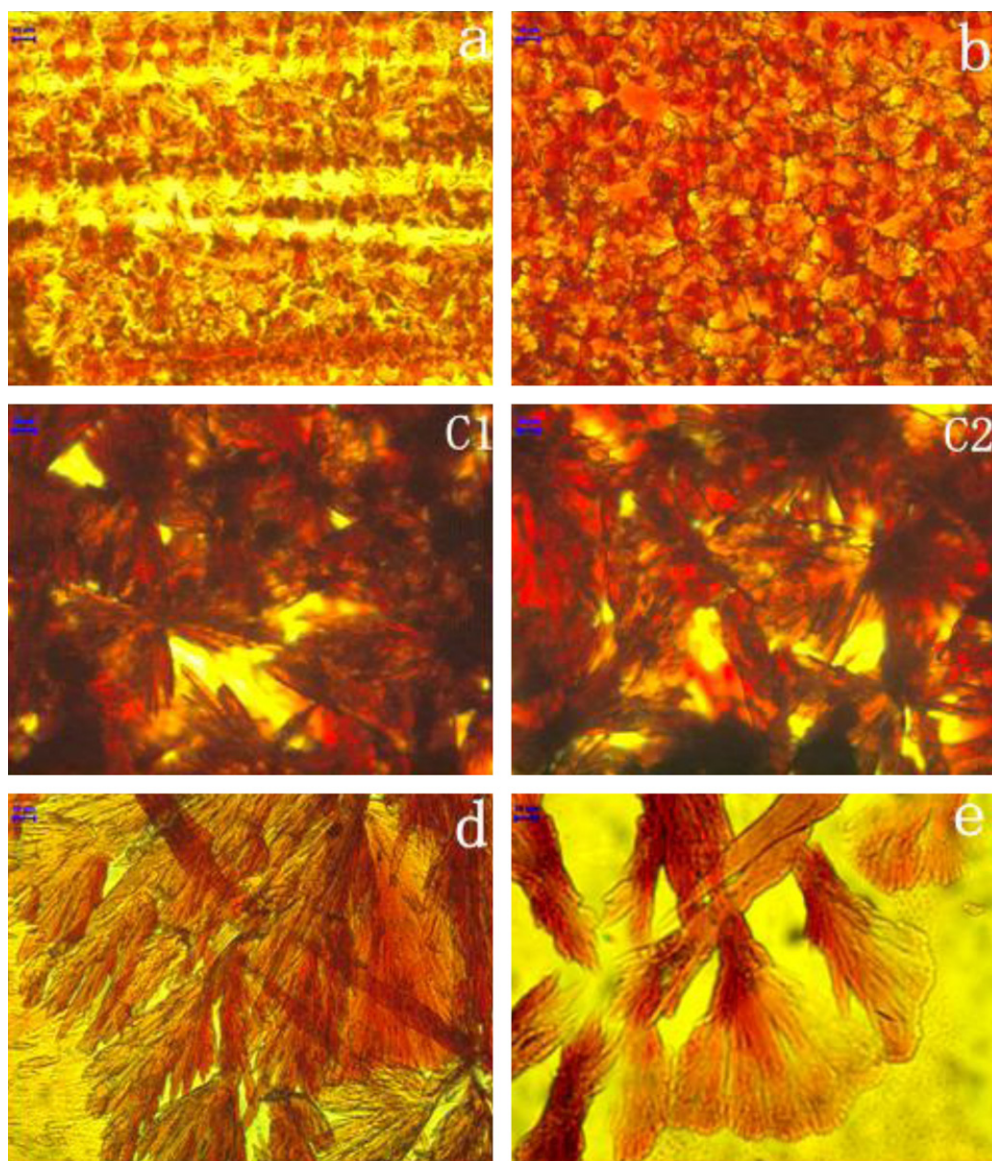

Fig. 7. Images of PoPD after the addition of SDS: (a)–(e) correspond to PoPD synthesized when the amounts of SDS added were 0.06, 0.08, 0.1, 0.12, and 0.14 g. Dimensional scale is 10 μm.
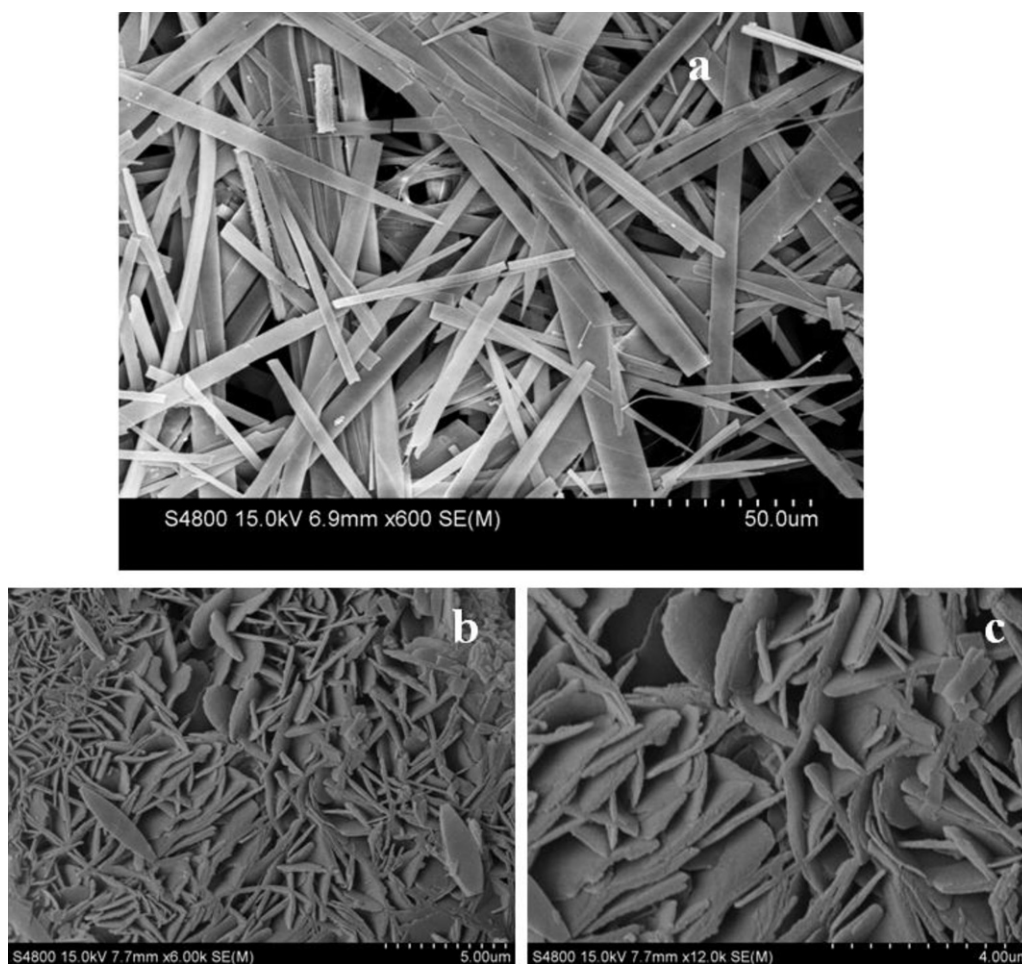
Fig. 8. (a) SEM image of the product without SDS; (b and c) SEM images of PoPD (c).

the peaks correspond to C=N and benzene ring of PoPD shifted to a lower wavenumber in Fig. 4c. This is caused by SO_3 in SDS. As an electron-withdrawing group, SO_3 decreased the density of electron cloud of the molecular chain and consequently reduced the inter-atomic force constants, thus the energy required for the electron transitions declined, leading to the shift of wavenumber to lower value. Besides, there are more peaks appear in Fig. 4c at 2900–2700 cm^{-1} which are attributable to C—H stretching vibration of —CH_3 and —CH_2 from SDS. Therefore, PoPD of 1,4-substituted benzenoid–quinoid structure were yielded both in the presence and absence of SDS [37,38].

3.4. UV–vis characterization

To further confirm the formation of the PoPD, UV–vis measurement was employed. The UV–vis results of surfactant-free PoPD are presented in Fig. 5a from which the major peaks of 285 and 427 nm are observed. The band at 427 nm is assigned to n–π^* transition associated with the phenazine ring conjugated to the two lone pairs of nitrogen. The other peak at about 285 is mainly ascribed to the π–π^* transition of the benzenoid and quinoid structures, and the peak shows a red shift compared with the value in the literature [39], further confirming the structure suggested by FT-IR characterization. The product of PoPD (c) was characterized by UV–vis and the result was shown in Fig. 5b. Two peaks were shown at 280 and 425 nm, which are similar to the result of Fig. 5a. In this characterization, the influence of the remaining SDS in the product is negligible. Above results suggest again that the structure

of product prepared in the presence of SDS is 1,4-substituted benzenoid–quinoid structure.

3.5. Effects of the surfactant

Surfactants could affect the synthesis process and the morphology of the materials. The influence of SDS concentration was investigated in this work. As is shown in Fig. 6, the product synthesized without SDS is uniformly dispersed one-dimensional structure with a width of about 2 μm. The monomers self-assembled on the surface of ITO glass slide and the rod-like material precipitated on the bottom of the solution, meanwhile the monomers on the glass surface continue to polymerize. Thus uniform dispersion of PoPD was obtained.

To study the effect of the amount of the surfactant concentration, different amounts of SDS were added before polymerization. As can be seen from Fig. 7, with the increase of the concentration of SDS, morphologies of the resulting products changed into mainly three structures. It could be explained by that when the concentration of SDS added is smaller than 10 times of critical micelle concentration (CMC), the micelles formed were generally spherical, but when the concentration of SDS is greater than 10 times of CMC, the micelles would change into non-spherical structures which could be ellipsoid, oblate spheroid, flat or rod shaped. When the amounts of SDS were 0.06 g and 0.08 g (Fig. 7a and b), the micelles formed were flat, and oPD gathered at the electrode surface to form the irregular flake. When the SDS concentration increased, the shape of the micelle was in a transition to the rod, thus the product
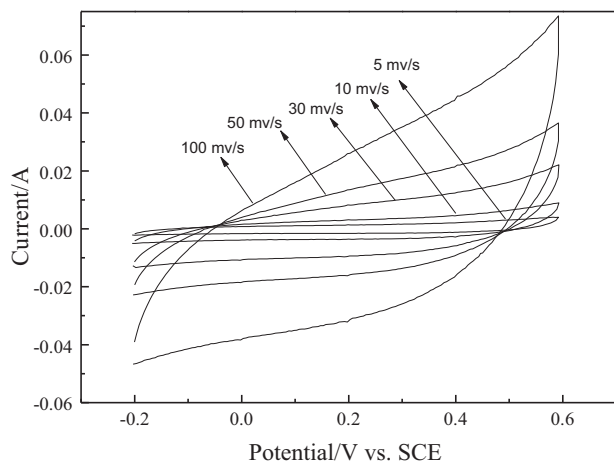
Fig. 9. Cyclic voltammograms of PoPD (c) recorded in 1.0 mol L^{-1} KNO$_3$ at various scan rates.

Fig. 10. Galvanostatic charge/discharge curves of PoPD (c) supercapacitor at various constant current densities.

obtained contained the rod-like structure (Fig. 7c). As the SDS concentration further increased (Fig. 7d, e), the rod-like structure accounted for a greater proportion in the PoPD with one end of rod and the other end of flat-shape. From the results, PoPD obtained in the presence of 0.1 g SDS is uniform, namely, PoPD (c) which was used for following characterizations and electrochemical measurements.

The products prepared without SDS (Fig. 8a) and with SDS (Fig. 8b and c) were characterized by SEM. As is shown in Fig. 8, the surfactant-free PoPD is microbelts with the width of 10 μm, and PoPD (c) has the petal-like and diamond-shaped structure, indicating that the addition of the surfactant greatly influenced the morphology of the products.

3.6. Electrochemical properties of PoPD

In the three-electrode system, cyclic voltammetry was employed to examine the electrochemical performance of PoPD (c). Fig. 9 shows the cyclic voltammogram obtained in the potential range of −0.2 to 0.6 V. No obvious redox peak shows, and the reason is that quasi-capacitive behavior is involved in this process, which is similar to double layer capacitor behavior with symmetrical shapes. The area of the curve increases with the scan rate. In the selected potential range, the specific capacitance could be calculated according to the following formula (1) [40]:

$$C = \frac{1}{m(V_2 - V_1)} \int_{V_1}^{V_2} \left(\frac{Q}{V}\right) dV = \frac{1}{m(V_2 - V_1)} \int_{V_1}^{V_2} \left(\frac{i}{v}\right) dV \qquad (1)$$

where V_1 and V_2 are the lower and upper potentials, respectively; v is the scan rate; m is the mass of active material. It was calculated that the specific capacitances are 106.4, 100.7, 97.5, 97.1, and 95.8 F g^{-1}, respectively at the scan rates of 5, 10, 30, 50 and 100 mV s^{-1}. As was determined by the GPC characterization, the molecular weight of PoPD (d) is 2596, namely, it has 24 oPD units which is higher than the PoPD prepared in previous work [28]. The long π-conjugated structure of the product may contribute largely to the capacity in this test. For electrochemical capacitors, the closer of its cyclic voltammogram shape to rectangle, the better capacitive property the active material bears. Cyclic voltammograms of PoPD synthesized in this experiment are not regular rectangular,
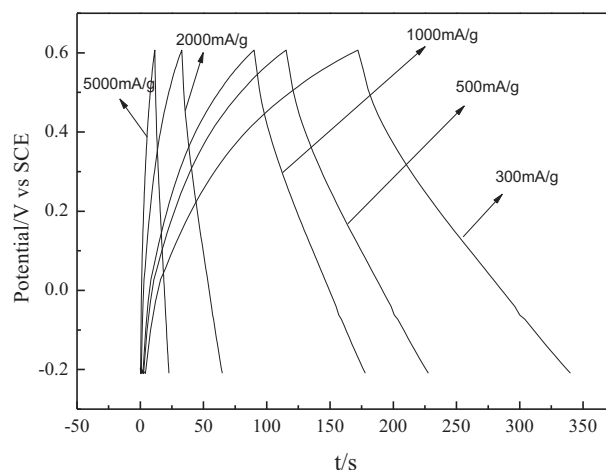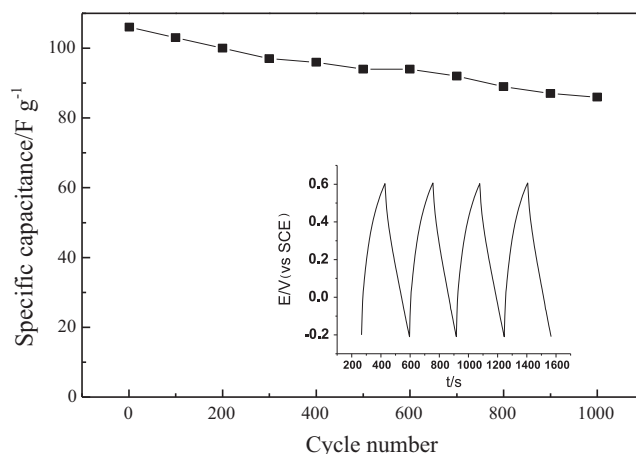

Fig. 11. Cycle life performance of the prepared supercapacitor in 1.0 mol L^{-1} KNO$_3$ solution; inset is charge–discharge curves at a galvanostatic current of 500 mA g^{-1}.

indicating the material is still to be explored for better capacitive behavior.

Charge/discharge curves of different current densities are given in Fig. 10, showing that the curves are like isosceles triangle, but a voltage drop shows in the early stage of the discharge due to the presence of the resistance of the electrode material, and the charge transfer resistance of the material is 6.58 Ω as measured by electrochemical impedance spectra. The time of charge/discharge process decreases with the increase of the current density. It is calculated that the specific capacitance at 500 mA g^{-1} is 105.6 F g^{-1} which is consistent with the result calculated from CV curve. To investigate the influence of the morphology of the capacitive behavior, the specific capacitance (SC) of the products were measured with CV in the potential range of −0.2 to 0.6 V at the scan rate of 5 mV s^{-1}, and the results are shown in Table 1 which suggests that the morphology change of the products caused by the addition of SDS posed certain influence on SC values.

To investigate the stability of the material applied in the capacitors, charge/discharge in 1.0 mol L^{-1} KNO$_3$ at the current density of 500 mA g^{-1} in the potential range of −0.2 to 0.6 V was conducted

Table 1
Specific capacitance of products synthesized with different addition of SDS.

	PoPD (surfactant free)	PoPD (a)	PoPD (b)	PoPD (c)	PoPD (d)	PoPD (e)
SC (F g^{-1})	73.2	84.9	85.3	106.4	105.1	90.4

for 1000 times. Fig. 11 shows the specific capacitance of the supercapacitor. It retained up to 82% of its original value at 1000th cycle, suggesting a good cycling stability of the as-prepared PoPD materials [41]. This might be ascribed to the good conductivity, permeability and electrochemical reversibility of PoPD materials. The flake structure whose specific surface area was measured to be 235.8 $m^2\,g^{-1}$, introduces electrostatic adsorption occurring at high current density, which is favorable for supercapacitor application [42].

4. Conclusions

PoPD microbelts were synthesized in neutral solution by CV technique in the potential range of 0–1 V at the scan rate of 50 mV s^{-1}. This method was also applied to prepare the petal-like and diamond-shaped PoPD material with the addition of SDS. When applied as electrode materials in supercapacitors, PoPD materials demonstrated a good electrochemical performance. The developed technique is a facile approach to prepare PoPD for supercapacitor applications.

Acknowledgements

References

[1] Y.T. Tsai, C.T. Lai, R.H. Chien, J.L. Hong, Thermal and spectral stability of electroluminescent hyper branched copolymers, Journal of Polymer Science Part A–Polymer Chemistry 50 (2012) 237.

[2] B. Kim, J. Kim, E. Kim, Visible to Near-IR Electrochromism and photothermal effect of poly(3,4-propylenedioxyselenophene)s, Macromolecules 44 (2011) 8791.

[3] R. Solmaz, E.A. Sahin, G. Karda, Electrochemical preparation and characterization of nickel and zinc-modified poly-2-aminothiazole films on mild steel surface and their corrosion inhibition performance, Reactive and Functional Polymers 71 (2011) 1148.

[4] J. Yano, A. Muta, Y. Harima, Poly(2,5-dimethoxyaniline) film coating for corrosion protection of iron, Journal of Solid State Electrochemistry 15 (2011) 601.

[5] X. Li, M. Huang, W. Duan, Novel multifunctional polymers from aromatic diamines by oxidative polymerization, Chemical Reviews 102 (2002) 2925.

[6] C. Ge, X. Yang, C. Li, B. Hou, Synthesis of polyaniline nanofiber and copolymerization with acrylate through in situ emulsion polymerization, Journal of Applied Polymer Science 123 (2012) 627.

[7] Z. Wang, F. Liao, S. Yang, T. Guo, A novel route synthesis of poly(orthophenylenediamine) fluffy microspheres self-assembled from nanospheres, Fibers and Polymers 12 (2011) 997.

[8] N. Larsona, K. Greish, H. Bauer, H. Maedad, H. Ghandehari, Synthesis and evaluation of poly(styrene-co-maleic acid) micellar nanocarriers for the delivery of tanespimycin, International Journal of Pharmaceutics 420 (2011) 111.

[9] F. Gonzaga, J.B. Grande, M.A. Brook, Morphology-controlled synthesis of poly(oxyethylene)silicone or alkylsilicone surfactants with explicit, atomically defined, branched, hydrophobic tails, Chemistry A European Journal 18 (2012) 1536.

[10] T.L.A Campos, D.F. Kersting, C.A. Ferreira, Chemical synthesis of polyaniline using sulphanilic acid as dopant agent into the reactional medium, Surface and Coatings Technology 122 (1999) 3.

[11] B. Bhowmick, M.K. Bain, D. Maity, N.K. Bera, D. Mondal, M.M.R. Mollick, Synthesis of dendritic polyaniline nanofibers by using soft template of sodium alginate, Journal of Applied Polymer Science 123 (2012) 1630.

[12] M. Canales, D. Aradilla, C. Aleman, Water absorption in polyaniline emeraldine base, Journal of Polymer Science, Part B: Polymer Physics 49 (2011) 1322.

[13] A.R. Elkaisa, M.M. Gvozdenovi, B.Z. Jugovi, J.S. Stevanovic, Electrochemical synthesis and characterization of polyaniline thin film and polyaniline powder, Progress in Organic Coatings 71 (2011) 32.

[14] X. Lu, H. Mao, D. Chao, X. Zhao, W. Zhang, Y. Wei, Preparation and characterization of poly(o-phenylenediamine) microrods using ferric chloride as an oxidant, Material Letters 61 (2007) 1400.

[15] Jaidev, S. Ramaprabhu, Poly(p-phenylenediamine)/graphene nanocomposites for supercapacitor applications, Journal of Materials Chemistry 22 (2012) 18775.

[16] Y. Chen, X. Zhang, H. Zhang, D. Sun, D. Zhang, Y. Ma, High-performance supercapacitors based on a graphene-activated carbon composite prepared by chemical activation, RSC Advances 2 (2012) 7747.

[17] L. Cai, H. Chen, Electrocatalytic reduction of hydrogen peroxide at platinum microparticles dispersed in a poly(o-phenylenediamine) film, Sensors and Actuators B 55 (1999) 14.

[18] S. Mu, The Electrocatalytic oxidative polymerization of o-phenylenediamine by reduced graphene oxide and properties of poly(o-phenylenediamine), Electrochimica Acta 56 (2011) 3764.

[19] J. Ping, J. Wu, K. Fan, Y. Ying, An amperometric sensor based on Prussian Blue and poly(o-phenylenediamine) modified glassy carbon electrode for the determination of hydrogen peroxide in beverages, Food Chemistry 126 (2011) 2005.

[20] P. Gajendran, R. Saraswathi, Enhanced electrochemical growth and redox characteristics of poly(o-phenylenediamine) on a carbon nanotube modified glassy carbon electrode and its application in the electrocatalytic reduction of oxygen, Journal of Physical Chemistry 111 (2007) 11320.

[21] S.S. Abd El Rehima, S.M. Sayyah, M.M. El–Deeb, S.M. Kamal, R.E. Azooz, Poly(o-phenylenediamine) as an inhibitor of mild steel corrosion in HCl solution, Materials Chemistry and Physics 123 (2010) 20.

[22] L. Wu, J. Luo, Z. Lin, Spectroelectrochemical studies of poly-o-phenylenediamine. Part 1. In situ resonance Raman spectroscopy, Journal of Electroanalytical Chemistry 417 (1996) 53.

[23] K. Martinusz, G. Láng, G. Inzelt, Impedance analysis of poly(o-phenylenediamine) electrodes, Journal of Electroanalytical Chemistry 433 (1997) 1.

[24] M. Ujvári, G. Láng, G. Inzelt, The problem of the low-frequency dispersion in the case of polymer film electrodes – an experimental impedance study on Au|poly(o-phenylenediamine) electrodes, Electrochemistry Communications 2 (2000) 497.

[25] Z. Wang, F. Liao, S. Yang, T. Guo, Synthesis of poly(o-phenylenediamine)/ferric oxide composites with rose-like hierarchical microstructures, Materials Letters 67 (2012) 121.

[26] X. Sun, M. Hagner, Mixing aqueous ferric chloride and o-phenylenediamine solutions at room temperature: a fast, economical route to ultralong microfibrils of assemblied o-phenylenediamine dimmers, Langmuir 23 (2007) 10441.

[27] L. Wang, S. Guo, S. Dong, Facile synthesis of poly(o-phenylenediamine) microfibrils using cupric sulfate as the oxidant, Material Letters 62 (2008) 3240.

[28] X. Sun, S. Dong, E. Wang, Large scale, templateless, surfactantless route to rapid synthesis of uniform poly(o-phenylenediamine) nanobelts, Chemical Communications 10 (2004) 1182.

[29] Y. Wang, Z. Liu, B. Han, Z. Sun, Y. Huang, G. Yang, Facile synthesis of polyaniline nanofibers using chloroauric acid as the oxidant, Langmuir 21 (2005) 833.

[30] C. Bian, H. Xiong, X. Zhang, W. Wen, S. Wang, An electrochemical biosensor for analysis of fenton-mediated oxidative damage to BSA using poly-o-phenylenediamine as electroactive probe, Biosensors and Bioelectronics 28 (2011) 216.

[31] D. Zane, A. Raffaele, A. Curulli, G.B. Appetecchi, S. Passerini, Electrosynthesis of poly(o-phenylenediamine) in a room temperature ionic liquid, Electrochemistry Communication 9 (2007) 2037.

[32] E.Y. Pisarevskaya, T.M. Serdyuk, E.V. Ovsyannikova, A.K. Buryak, N.M. Alpatova, Electropolymerization features of o-phenylenediamine on carbon electrode with developed surface, Synthetic Metals 160 (2010) 2366.

[33] D. Chirizzi, C. Malitesta, Potentiometric urea biosensor based on urease immobilized by an electrosynthesized poly(o-phenylenediamine) film with buffering capability, Sensors and Actuators B 157 (2011) 211.

[34] A. Prună, F. Brânzoi, Electrochemical activity and microscopy of electrosynthesised poly(o-phenylenediamine) nanotubes, Journal of Polymer Research 19 (2012) 9879.

[35] P. Muthirulan, N. Rajendran, Poly(o-phenylenediamine) coatings on mild steel: electrosynthesis, characterization and its corrosion protection ability in acid medium, Surface & Coatings Technology 206 (2012) 2072.

[36] S. Youssef, K. Dalila, A. Ridha, Electropolymerization of phenol, o-nitrophenol and o-methoxyphenol on gold and carbon steel materials and their corrosion protection effects, Progress in Organic Coatings 69 (2010) 335.

[37] J. Han, Y. Liu, L. Li, R. Guo, Poly(o-phenylenediamine) submicrosphere-supported gold nanocatalysts: synthesis, characterization, and application in selective oxidation of benzyl alcohol, Langmuir 25 (2009) 11054.

[38] J. Han, J. Dai, R. Guo, Highly efficient adsorbents of poly(o-phenylenediamine) solid and hollow sub-microspheres towards lead ions: a comparative study, Journal of Colloid and Interface Science 356 (2011) 749.

[39] X. Sun, S. Dong, E. Wang, Formation of o-phenylenediamine oligomers and their self-assembly into one-dimensional structures in aqueous medium, Macromolecular Rapid Communication 26 (2005) 1504.

[40] C. Shen, X. Wang, W. Zhang, F. Kang, A high-performance three-dimensional micro supercapacitor based on self-supporting composite materials, Journal of Power Sources 196 (2011) 10465.

[41] G. Wang, L. Zhang, J. Zhang, A review of electrode materials for electrochemical supercapacitors, Chemical Society Reviews 41 (2012) 797.

[42] T. Yousefi, A.N. Golikand, M.H. Mashhadizadeh, M. Aghazadeh, High temperature and low current density synthesis of Mn_3O_4 porous nano spheres: characterization and electrochemical properties, Current Applied Physics 12 (2012) 544.